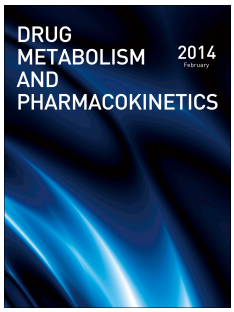

Novel variants in outer protein surface of flavin-containing monooxygenase 3 found in an Argentinian case with impaired capacity for trimethylamine *N*-oxygenation

Leonardo Dionisio, Makiko Shimizu, Sofia Stupniki, Saki Oyama, Eugenio Aztiria, Maximiliano Alda, Hiroshi Yamazaki, Guillermo Spitzmaul

PII: S1347-4367(20)30365-7

DOI: https://doi.org/10.1016/j.dmpk.2020.05.003

Reference: DMPK 331

To appear in: *Drug Metabolism and Pharmacokinetics*

Received Date: 29 February 2020

Revised Date: 22 April 2020

Accepted Date: 5 May 2020

Please cite this article as: Dionisio L, Shimizu M, Stupniki S, Oyama S, Aztiria E, Alda M, Yamazaki H, Spitzmaul G, Novel variants in outer protein surface of flavin-containing monooxygenase 3 found in an Argentinian case with impaired capacity for trimethylamine *N*-oxygenation, *Drug Metabolism and Pharmacokinetics* (2020), doi: https://doi.org/10.1016/j.dmpk.2020.05.003.

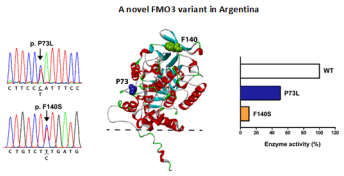

Novel variants in outer protein surface of flavin-containing monooxygenase 3 found in an Argentinian case with impaired capacity for trimethylamine *N*-oxygenation

Leonardo Dionisio[a,b], Makiko Shimizu[c], Sofia Stupniki[a,b], Saki Oyama[c], Eugenio Aztiria[a,b], Maximiliano Alda[d], Hiroshi Yamazaki [c,*], and Guillermo Spitzmaul[a,b,*]

[a] Instituto de Investigaciones Bioquímicas de Bahía Blanca (INIBIBB)-Consejo Nacional de Investigaciones Científicas y Técnicas (CONICET)/Universidad Nacional del Sur (UNS). B8000FWB, Bahía Blanca, Argentina.

[b] Departamento de Biología, Bioquímica y Farmacia (BByF), UNS. B8000ICN, Bahía Blanca, Argentina.

[c] Laboratory of Drug Metabolism and Pharmacokinetics, Showa Pharmaceutical University. Machida, Tokyo 194-8543, Japan.

[d] Instituto de Diagnóstico Infantil (IDDI). B8000CLO, Bahía Blanca, Argentina.

Running title: A novel FMO3 variant in Argentina

* **Corresponding authors**:

Showa Pharmaceutical University, 3-3165 Higashi-tamagawa Gakuen, Machida, Tokyo 194-8543, Japan. Tel.: +81 42 721 1406; fax: +81 42 721 1406. E-mail address: hyamazak@ac.shoyaku.ac.jp (H. Yamazaki)

Or

INIBIBB-CONICET/UNS, Camino La Carrindanga Km 7, 8000 Bahía Blanca, Argentina. Tel.: +54 291 4861201 (127); fax: +54 291 4861200. E-mail address: gspitz@inibibb-conicet.gob.ar (G. Spitzmaul)

Abstract

Flavin-containing monooxygenase 3 (FMO3) is a polymorphic drug metabolizing enzyme associated with the genetic disorder trimethylaminuria. We phenotyped a white Argentinian 11-year-old girl by medical sensory evaluation. After pedigree analysis with her brother and parents, this proband showed to harbor a new allele p.(P73L;E158K;E308G) *FMO3* in *trans* configuration with the second new one p.(F140S) *FMO3*. Recombinant FMO3 proteins of the wild-type and the novel two variants underwent kinetic analyses of their trimethylamine *N*-oxygenation activities. P73L;E158K;E308G and F140S FMO3 proteins exhibited moderately and severely decreased trimethylamine *N*-oxygenation capacities (~50% and ~10% of wild-type FMO3, respectively). Amino acids P73 and F140 were located on the outer surface region in a crystallographic structure recently reported of a FMO3 analog. Changes in these positions would indirectly impact on key FAD-binding residues. This is the first report and characterization of a patient of fish odor syndrome caused by genetic aberrations leading to impaired FMO3-dependent *N*-oxygenation of trimethylamine found in the Argentinian population. We found novel structural determinants of FAD-binding domains, expanding the list of known disease-causing mutations of FMO3. Our results suggest that individuals homozygous for any of these new variants would develop a severe form of this disorder.

Keywords: fish odor syndrome; FMO3; trimethylamine *N*-oxide

1. Introduction

Flavin-containing monooxygenases (FMOs) belong to a family of well conserved enzymes that are present in all living beings [1]. These monooxygenases are protecting enzymes that catalyze the *N*-oxygenation of a variety of nucleophilic organic nitrogen and sulfur compounds present in many drugs, pesticides, dietary components and other foreign compounds [2, 3]. To date, five functional *FMO* genes (*FMO1-FMO5*) and six pseudogenes (*FMO6P-FMO11P*) have been identified in humans [4, 5]. From these, FMO1, FMO3 and FMO5 are reportedly relevant to hepatic function [2, 3, 6]. The developmental maturation of FMO5 still remains controversial [7]. FMO1 is highly expressed during the fetal period and progressively decreases to undetectable levels after birth. By contrast, FMO3 expression onsets at the time of birth and increases over time, reaching an adult level during adolescence [8]. Crystal structures for analogs of vertebrate FMOs were recently described [9]. All FMOs enzymes, from bacteria to vertebrates, are dimers [9-11] but only the mammalian versions are ER anchored-membrane proteins due to an additional transmembrane α-helix domain [9]. FAD and NADPH binding sites are located deep into the structure of the protein [9]. The substrates have to navigate through protein tunnels to reach the catalytic area. Most residues in the active site and the cofactor binding-domain are conserved among a wide range of phyla [9-12]. Mutations in several of these residues affect the catalytic activity of the enzyme [12].

More than 30 different mutations and around 40 polymorphisms of *hFMO3* have been reported so far [13]. Many of these have been associated with a metabolic disorder known as trimethylaminuria (TMAU) [14, 15]. TMAU or “fish odor syndrome” is a non-life-

threatening condition arising from the altered or incomplete expression of the *FMO3* isoform. Under this condition, the volatile trimethylamine derived from dietary intake or produced by normal gut flora, typically with a decaying fish-like smell, is unable to be converted into the non-odorous trimethylamine *N*-oxide. Trimethylamine accumulation is then excreted through sweat, urine, breath and other body fluids [16, 17].

The impaired polymorphic variants of FMO3 responsible for TMAU have been mainly determined [18]. Genetic testing is a useful tool to understand the molecular basis of the condition and to detect heterozygous carriers. In this report, we describe a case of a white Argentinian 11-year-old girl undergoing progressive body malodor. TMAU was suspected and genetic testing was performed in all family members. To our knowledge, there are no previous published reports on TMAU genetic characterization in the Argentinian population.

2. Materials and methods

2.1 Ethics statement

Written informed consent for genetic explorations and the authorization for publication of the results of this study were obtained from the patient and her family in Instituto de Investigaciones Bioquímicas de Bahía Blanca. This study was conducted under the approval by the ethics committee of Showa Pharmaceutcal University in accordance with the Declaration of Helsinki.

2.2 Molecular analyses

FMO3 gene was sequenced and screened for mutations in the proband and her direct family members. Genomic DNA of all the concerned individuals was obtained from jaw swabs using the commercial kit DNA Puriprep S-kit (Inbio Highway). All of the *FMO3* coding exons (*i.e.* exons 2 to 9) were amplified from genomic DNA by polymerase chain reaction (PCR) using the primer pairs shown in Table 1. PCR products were separated in agarose gels and DNA was extracted and purified using a commercial kit (PB-L). Purified DNA was sequenced using an external service (Macrogen Inc., Korea). To ensure fidelity, readings were performed on both directions. DNA alignments and polymorphism detection were carried out online using the Blast application at the NCBI website as well as other software programs (i.e. SnapGene). The sequence of the complete human *FMO3* gene described in GenBank (Accession Number NG_012690.1) was used as reference.

2.3 DNA constructs and heterologous expression

Wild-type and variant *FMO3* cDNAs were prepared as previously described [19]. Site-directed mutagenesis was carried out using a QuikChange II Site-Directed Mutagenesis Kit (Stratagene, La Jolla, CA, USA) to prepare the following variant FMO3 proteins. Wild-type and modified FMO3 cDNAs were introduced into the pTrc99A expression vector (Pharmacia Biotechnology, Milwaukee, MI, USA) and then transformed into *Escherichia coli* strain JM109, as described previously [19]. The entire coding regions of the wild-type and mutagenized FMO3 cDNAs were verified by resequencing both strands with specific primers (Table 1). Bacterial membrane fractions expressing FMO3 were prepared from bacterial pellets after centrifugation as previously described [19]. The amounts of recombinant FMO3 (0.012–0.16 nmol FMO3/mg bacterial protein) were determined by immunochemical quantification using an anti-FMO3 antibody (ab126790, Abcam,

Cambridge, UK) and comparing the results with those of a recombinant human FMO3 standard (Corning), as reported previously [19].

2.4 Enzyme functional assays

Trimethylamine *N*-oxygenation rates were evaluated as described previously [19]. Briefly, a typical incubation mixture consisted of bacterial membranes (10 pmol equivalent FMO3) fortified with an NADPH-generating system (0.25 mM $NADP^+$, 2.5 mM glucose 6-phosphate, and 0.25 units/mL glucose 6-phosphate dehydrogenase) and 0–1000 μM trimethylamine in a final volume of 0.10 mL of 50 mM potassium phosphate buffer (pH 8.4, [20]). Incubations were carried out at 37°C for 10 min and terminated. Product formation was found to be linear up to 20 pmol of all FMO3 proteins and for 20 min. Deuterium-labeled trimethylamine-d_9 and trimethylamine *N*-oxide-d_9 were used as internal standards. After centrifugation (4°C, 20,000 × *g*, 10 min), metabolite concentrations in the transferred supernatants were determined using liquid chromatography/tandem mass spectrometry [21]. The detection limit of trimethylamine *N*-oxide was 10 nM under the present conditions.

Kinetic analyses of *N*-oxygenation of trimethylamine mediated by recombinant human FMO3 proteins were carried out in a nonlinear regression analysis using Prism software (GraphPad Software, San Diego, CA, USA).

2.5. Structural analysis of human FMO3

For the structural analysis of the enzyme we used the recently reported crystallographic dimer of AncFMO3-6 protein (PDB 6SE3) as a model for human FMO3 [9]. We analyzed molecular interactions and residue positions using the Discovery Studio Visualizer Client v4.1.0.14169 2014 (Accelrys Software Inc.).

3. Results

3.1. Case description. The proband is an Argentinian girl, that was 11 years old at the time of the first consultation to the physician. Her mother reported the girl produced increasingly body malodor, especially after the intake of choline-rich meals such as eggs, red meat, fish and milk, among others. The situation became a strong cause of social stress, isolation and suffering for the girl. The patient is the first child of healthy, unrelated parents; and her brother, 2 years younger, is apparently healthy. All the hematological parameters and biochemical indexes for renal, thyroid and liver function were within the normal range. The medical history of the patient showed that she underwent surgery for a thyroglossal duct cyst at the age of 9 month. She also presented an episode of atopic dermatitis.

TMAU was suspected and nutritional treatment was implemented immediately with restriction of choline-rich foods. This intervention greatly improved the main clinical symptom by reducing body malodor. Additionally, a genetic test was recommended to check out the presence of mutations in her *FMO3* gene. Trimethylamine levels in urine were not measured for two reasons, first, because these determinations are not available among the routine clinical laboratory techniques in Argentina and, second, the family did not authorize the study since an overdose of choline-rich foods in her diet would expose her to a strong distressing situation.

3.2 Gene analysis of the proband. Exon analysis of the *FMO3* gene in the proband revealed the presence of two polymorphisms already reported in the literature:

NG_012690.1:g.21949 G>A p.(E158K) in exon 4, resulting in a glutamic acid to lysine exchange (rs2266782) and NG_012690.1:g.28225 A>G p.(E308G) in exon 7, resulting in a glutamic acid to glycine exchange (rs2266780) (Fig. 1A). Additionally, the proband carried two unreported variations: NG_012690.1:g.17994 C>T p.(P73L) in exon 3, resulting in a proline to leucine substitution and NG_012690.1:g.21896 T>C p.(F140S) in exon 4, resulting in a phenylalanine to serine substitution (Fig. 1B). The proband resulted heterozygous for all the detected changes.

3.3 Pedigree analysis. In order to study the genetic status of the proband relatives and the putative origin of her genetic configuration, the *FMO3* genes of her brother and parents were evaluated. The analysis of the mother DNA revealed that she was carrying the newly detected mutation p.(P73L) in exon 3, plus the p.(E158K) and the p.(E308G) substitutions in exons 3 and 4, respectively. All changes were heterozygous. In consequence, substitution p.(P73L) was in *cis* configuration with p.(E158K) and p.(E308G) (Fig. 2). Examination of the father DNA showed that he was carrying the p.(F140S) substitution in exon 4 in heterozygosity with a wild allele (Fig. 2). Finally, her brother did not show any variations in his *FMO3* gene sequence. Thus, pedigree analysis of the proband revealed that the new allele p.(P73L;E158K;E308G) *FMO3* was in *trans* configuration with the second new allele, p.(F140S) *FMO3*. Therefore, she was a compound heterozygous for the two new alleles (Fig. 2).

3.4 *In vitro* FMO3 activity of the detected polymorphisms. Since the proband was the only member of the family that manifested a TMAU-like phenotype and in order to understand the contribution of each new *FMO3* allele to the catalytic function, we analyzed the

activities of the recombinant enzymes carrying the detected variants. The new p.(P73L;E158K;E308G) and p.(F140S) FMO3 proteins were separately expressed in bacterial membranes. As shown in Fig. 3A, the amounts of recombinant two FMO3 variants (0.012 nmol FMO3/mg bacterial protein) were ~one tenth of that of FMO3 wild-type (0.16 nmol FMO3/mg bacterial protein) determined by immunochemical quantification. Under the present condition, wild-type FMO3 showed K_{cat} and K_m values of 54 ± 2 nmol/min/nmol FMO3 and 40 ± 5 μM (with 1.4 $\mu M^{-1}min^{-1}$ of k_{cat}/K_m value; Fig. 3B). The FMO3 variants resulting from the combination of P73L;E158K;E308G and of F140S showed K_{cat} and K_m values of 27 ± 1 nmol/min/nmol FMO3 and 24 ± 4 μM (with 1.1 $\mu M^{-1}min^{-1}$ of k_{cat}/K_m) and K_{cat} and K_m values of 4 ± 1 nmol/min/nmol FMO3 and 16 ± 3 μM (with 0.25 $\mu M^{-1}min^{-1}$ of k_{cat}/K_m), respectively (Fig, 3B).

3.5 Structure-function correlation. To get insights into the molecular consequences of P73L and F140S substitutions, we analyzed residue positions and interactions in the protein structure. We used the recently reported crystal structure of AncFMO3-6 (PDB 6SE3), as it was recently proposed as a structural model for human FMO3 [22]. None of the changed residues can directly interact with ligands or participate in the active site (Fig. 4A). Besides they do not participate in the dimerization domain (inner face of the monomer). Additional substitutions observed in one allele (E158K, E308G) are neither close to P73 position, suggesting independent structural alterations of the protein. All these four residues are exposed to the outer protein surface and far from the membrane-protein interface (Fig. 4A).

In order to understand the structural alterations that these mutations could potentially introduce, we closer studied the molecular interactions of these residues. P73 is placed in a

random structure that connects α-helix 3 and 4, facing the outer surface of the protein. This residue is located outside the active site, just behind the isoalloxazine ring of FAD. It is surrounded by α-helix 3, 4, 21 and 22 (Fig. 4B, left). Before the α-helix 3, there are two residues that interact with the isoalloxazine ring, N61 (OD1 with FAD O4) and S62 (OG with FAD N3). Multiple hydrophobic interactions and one H-bond are observed in this region that could link P73 with these two residues interacting with FAD, so far P73-T469, Y469-C68, C68-Y74, Y74-M67 and M67-S62 (Fig. 4B, right). Besides most of these residues establish several interactions with one or more other residues, as is the case for both Y.

F140 is located in the 6th β–sheet, being part of a hydrophobic core. Similar to *Schizosaccharomyces pombe* FMO (sFMO) [23], in the ancFMO3-6 model, this core is formed by an inner wall composed of a five-stranded parallel β-sheet and an outer wall which is structured by a three-stranded antiparallel β-sheet (Fig. 4C). The inner wall makes contact with N1' and N6' of the adenosine group of the FAD through V110 (equivalent to V138 that interacts with the adenosine group in sFMO) (Fig 4C). Phenyl group of F140 protrudes into the middle of the hydrophobic core (Fig. 4C). All the residues forming the core are aliphatic: A6, I8, T29, F31, V110, V113, W125, V127, T129, A138, F140, V143 and I145 (Fig. 4c, right).

4. Discussion

In this study, we evaluated an 11-year-old Argentinian girl with clinical suspicion of TMAU. Our molecular genetic studies revealed that she was heterozygous for four polymorphisms. Two of them, E158K and E308G, are relatively common SNPs, known to cause a mild

reduction in FMO3 enzymatic activity [14, 24-28]. Because her father carried the F140S mutation and the mother carried the P73L, E158K and E308G mutations, we deduced the proband is a compound heterozygote for the polymorphisms with mutations P73L, E158K and E308G in the *cis* configuration while the F140S is in the second allele. In consequence, the proband expresses enzyme dimers that could either be composed of two identical monomers p.(P73L;E158K;E308G) or p.(F140S), or a combination of both. *In vitro* expression of these alleles exhibited a reduced metabolic capacity by 50% and 90%, respectively, compared to the wild-type FMO3 (Fig. 3). Proband parents did not show a TMAU-like phenotype, since they carry a wild-type *FMO3* allele which would guarantee the proper trimethylamine metabolization.

Several studies have reported that the E158K polymorphism leads to a reduced FMO3 catalytic activity, which appears to vary, depending on the substrate [29, 30]. Previous *in vitro* expression studies showed that the K158 mutant form of the protein is a poorer trimethylamine *N*-oxygenator than the E158 form. When this mutation is combined with the E308G mutation on the same allele, results in an even more pronounced effect on FMO3 function. However this combination slightly decreases enzyme activity (about 25%) [18]. These two FMO3 mutations have a relative high frequency in European population (0.420 for E158K and 0.217 for E308G)[18]. Additionally, we report here two novel mutations, P73L and F140S, each of them causing a strong decrease in enzyme activity when they were evaluated in heterologous expression (more than 90% for F140S and about 50% for P73L). In the case of the proband, by having a combination of two defective alleles, FMO3 activity would have, in the best case, a 50% decrease, with a probability of 0.25, according to dimer

assembly or a 90% decrease with the same probability. The combination of both alleles, with a probability of 0.5, would decrease the activity of the enzyme in between 50 to 90%.

Taking into consideration the genetic analysis and the improvement of the symptomatology after attaching to a choline-free diet, TMAU is strongly suggested in the proband, despite not having had the chance to test her metabolic capacity. TMAU is classified into severe (<60%) or mild (60-90%) according to metabolic capacity defined as the ratio of trimethylamine *N*-oxide to total trimethylamine in urine [31, 32]. Clinical symptoms in the proband were very strong even with a small consumption of choline-rich foods, such as eggs or soy products. In accordance, the expected decreased in FMO3 activity will always be in the range of 50% or lower, so this patient could be classified into the severe form of TMAU.

All classical TMAU-causing mutations target residues located either in the active site or in structurally relevant regions [23, 33]. Indeed, the residues that most reduce the activity of the enzyme are near the surface in the structure [12]. According to this, P73 and F140 are residues which are not located at the active site of FMO3, but close to the cofactor binding domain. P73 is not in direct contact with FAD but is part of a net residues that through hydrophobic and H-bond interactions, contact with the FAD molecule. Probably the change of a proline by leucine results in the alteration of the interaction-balance with FAD, decreasing enzyme activity. Similar consequences are observed for the P70 position. This residue is located in the same loop and the change P70L showed a ~50% decreased enzyme activity among Japanese population [34]. Besides, residues that participate in the interaction network between N61-S62 and P73 (Fig. 4), such as K64, E65, M66 are reported

to abolish enzyme activity [12]. F140 is located in a hydrophobic core that delimits the adenine binding-site of the FAD molecule, which interacts with adenine through V110 (V138 in *S. pombe*) establishing two H-bond with it [22, 23], (Fig. 4C). We detected a mutation that changes a hydrophobic amino acid for a polar one (F140S). We speculate that this change may disrupt the non-polar core, and then, would alter the interactions with the adenosine ring of the cofactor FAD. Given that F140S generates a strong decrease in enzyme activity, our results show that interactions with adenosine ring, which do not participate in the active zone, could alter the optimal disposition of the isoalloxazine ring in the active site. To date, only one mutation (E32K) that also interacts with the adenosine ring, has been reported to abolish enzyme activity [35]. One mutation in this hydrophobic core was reported related to a TMAU case [36]. The hydrophobic core collectively seems to be important for proper orientation of the adenosine ring and its alteration may impair enzyme function.

In conclusion, we report here two novel mutations of FMO3 which are involved in a strong decrease of its metabolic capacity. In the proband, the combination of these novel mutations affecting both alleles, as a compound heterozygous, leads her to develop a “Fish Odor Syndrome”. *FMO3* gene expression is expected to increase from childhood to puberty, worsening fish odor production [37], as is the case of the patient reported here. Due to the impossibility to measure trimethylamine levels in urine, we can only infer that the proband shows a TMAU-like syndrome, because she presents body malodor and mutations in *FMO3* gene that drastically impair enzymatic function. The case is the first reported in Argentina. The fact that urine trimethylamine determinations are not routinely performed in clinical

laboratories in Argentina, contributes to the relative underestimation of TMAU in this country.

Conflict of interest

The authors declare that there are no conflicts of interest.

Author Contributions

(1) Study conception and design; E.A., L.D., H.Y. and G.S.

(2) Acquisition, analysis and/or interpretation of data; L.D., M.S., S.S., S.O., E.A., M.A., H.Y. and G.S.

(3) Drafting/revision of the work for intellectual content and context; E.A., L.D., S.S., H.Y. and G.S.

(4) Final approval and overall responsibility for the published work. H.Y. and G.S.

Acknowledgment

This work was supported by grants from Secretaría de Políticas Universitarias (VT38-UNS8614) to G.S., Universidad Nacional del Sur (PGI N24/B269) to E.A./G.S., and in part by the Japan Society for the Promotion of Science Grants-in-Aid for Scientific Research (19K07205) to M.S.

References

[1] Mascotti ML, Lapadula WJ, Juri Ayub M. The Origin and Evolution of Baeyer-Villiger Monooxygenases (BVMOs): An Ancestral Family of Flavin Monooxygenases. PloS one 2015;10(7):e0132689.

[2] Cashman JR, Zhang J. Human flavin-containing monooxygenases. Annual review of pharmacology and toxicology 2006;46:65-100.

[3] Krueger SK, Williams DE. Mammalian flavin-containing monooxygenases: structure/function, genetic polymorphisms and role in drug metabolism. Pharmacology & therapeutics 2005;106(3):357-87.

[4] Hernandez D, Janmohamed A, Chandan P, Phillips IR, Shephard EA. Organization and evolution of the flavin-containing monooxygenase genes of human and mouse: identification of novel gene and pseudogene clusters. Pharmacogenetics 2004;14(2):117-30.

[5] Hines RN, McCarver DG. The ontogeny of human drug-metabolizing enzymes: phase I oxidative enzymes. The Journal of pharmacology and experimental therapeutics 2002;300(2):355-60.

[6] Mitchell SC. Flavin mono-oxygenase (FMO)--the 'other' oxidase. Current drug metabolism 2008;9(4):280-4.

[7] Chen Y, Zane NR, Thakker DR, Wang MZ. Quantification of Flavin-containing Monooxygenases 1, 3, and 5 in Human Liver Microsomes by UPLC-MRM-Based Targeted Quantitative Proteomics and Its Application to the Study of Ontogeny. Drug Metab Dispos 2016;44(7):975-83.

[8] Koukouritaki SB, Simpson P, Yeung CK, Rettie AE, Hines RN. Human hepatic flavin-containing monooxygenases 1 (FMO1) and 3 (FMO3) developmental expression. Pediatric research 2002;51(2):236-43.

[9] Nicoll CR, Bailleul G, Fiorentini F, Mascotti ML, Fraaije MW, Mattevi A. Ancestral-sequence reconstruction unveils the structural basis of function in mammalian FMOs. Nat Struct Mol Biol 2020;27(1):14-24.

[10] Alfieri A, Malito E, Orru R, Fraaije MW, Mattevi A. Revealing the moonlighting role of NADP in the structure of a flavin-containing monooxygenase. ProcNatlAcadSciUSA 2008;105(18):6572-7.

[11] Eswaramoorthy S, Bonanno JB, Burley SK, Swaminathan S. Mechanism of action of a flavin-containing monooxygenase. Proceedings of the National Academy of Sciences 2006;103:9832-7.

[12] Chhibber-Goel J, Singhal V, Gaur A, Yogavel M, Sharma A. Structure–Function Analysis of Liver Flavin Monooxygenase 3 that Drives Trimethylaminuria in Humans. Proceedings of the National Academy of Sciences, India Section B: Biological Sciences 2018;88(4):1681-90.

[13] Phillips IR, Shephard EA. Flavin-containing monooxygenase 3 (FMO3): genetic variants and their consequences for drug metabolism and disease. Xenobiotica 2020;50(1):19-33.

[14] Shephard EA, Treacy EP, Phillips IR. Clinical utility gene card for: Trimethylaminuria - update 2014. European journal of human genetics : EJHG 2015;23(9).

[15] Motika MS, Zhang J, Zheng X, Riedler K, Cashman JR. Novel variants of the human flavin-containing monooxygenase 3 (FMO3) gene associated with trimethylaminuria. Molecular genetics and metabolism 2009;97(2):128-35.

[16] Mackay RJ, McEntyre CJ, Henderson C, Lever M, George PM. Trimethylaminuria: causes and diagnosis of a socially distressing condition. The Clinical biochemist Reviews 2011;32(1):33-43.

[17] Mitchell SC. Trimethylaminuria (fish-odour syndrome) and oral malodour. Oral diseases 2005;11 Suppl 1:10-3.

[18] Yamazaki H, Shimizu M. Survey of variants of human flavin-containing monooxygenase 3 (FMO3) and their drug oxidation activities. Biochemical pharmacology 2013;85(11):1588-93.

[19] Shimizu M, Yoda H, Nakakuki K, Saso A, Saito I, Hishinuma E, et al. Genetic variants of flavin-containing monooxygenase 3 (FMO3) derived from Japanese subjects with the trimethylaminuria phenotype and whole-genome sequence data from a large Japanese database. Drug Metab Pharmacokinet 2019;34(5):334-9.

[20] Nagashima S, Shimizu M, Yano H, Murayama N, Kumai T, Kobayashi S, et al. Inter-individual variation in flavin-containing monooxygenase 3 in livers from Japanese: correlation with hepatic transcription factors. Drug Metab Pharmacokinet 2009;24(3):218-25.

[21] Shimizu M, Yamazaki H. Human plasma and urinary metabolic profiles of trimethylamine and trimethylamine N-oxide extrapolated using a simple physiologically based pharmacokinetic model. J Toxicol Sci 2017;42(4):485-90.

[22] Nicoll CR, Bailleul G, Fiorentini F, Mascotti ML, Fraaije MW, Mattevi A. Ancestral-sequence reconstruction unveils the structural basis of function in mammalian FMOs. Nature structural & molecular biology 2019.

[23] Eswaramoorthy S, Bonanno JB, Burley SK, Swaminathan S. Mechanism of action of a flavin-containing monooxygenase. Proceedings of the National Academy of Sciences of the United States of America 2006;103(26):9832-7.

[24] Shimizu M, Origuchi Y, Ikuma M, Mitsuhashi N, Yamazaki H. Analysis of six novel flavin-containing monooxygenase 3 (FMO3) gene variants found in a Japanese population suffering from trimethylaminuria. Molecular genetics and metabolism reports 2015;5:89-93.

[25] Shimizu M, Yano H, Nagashima S, Murayama N, Zhang J, Cashman JR, et al. Effect of genetic variants of the human flavin-containing monooxygenase 3 on N- and S-oxygenation activities. Drug metabolism and disposition: the biological fate of chemicals 2007;35(3):328-30.

[26] Koukouritaki SB, Poch MT, Cabacungan ET, McCarver DG, Hines RN. Discovery of novel flavin-containing monooxygenase 3 (FMO3) single nucleotide polymorphisms and functional analysis of upstream haplotype variants. Molecular pharmacology 2005;68(2):383-92.

[27] Dolphin CT, Janmohamed A, Smith RL, Shephard EA, Phillips IR. Missense mutation in flavin-containing mono-oxygenase 3 gene, FMO3, underlies fish-odour syndrome. Nature genetics 1997;17(4):491-4.

[28] Treacy EP, Akerman BR, Chow LM, Youil R, Bibeau C, Lin J, et al. Mutations of the flavin-containing monooxygenase gene (FMO3) cause trimethylaminuria, a defect in detoxication. Human molecular genetics 1998;7(5):839-45.

[29] Lattard V, Zhang J, Tran Q, Furnes B, Schlenk D, Cashman JR. Two new polymorphisms of the FMO3 gene in Caucasian and African-American populations: comparative genetic and functional studies. Drug metabolism and disposition: the biological fate of chemicals 2003;31(7):854-60.

[30] Park CS, Kang JH, Chung WG, Yi HG, Pie JE, Park DK, et al. Ethnic differences in allelic frequency of two flavin-containing monooxygenase 3 (FMO3) polymorphisms: linkage and effects on in vivo and in vitro FMO activities. Pharmacogenetics 2002;12(1):77-80.

[31] Shimizu M, Allerston CK, Shephard EA, Yamazaki H, Phillips IR. Relationships between flavin-containing mono-oxygenase 3 (FMO3) genotype and trimethylaminuria phenotype in a Japanese population. British journal of clinical pharmacology 2014;77(5):839-51.

[32] Motika MS, Zhang J, Cashman JR. Flavin-containing monooxygenase 3 and human disease. Expert opinion on drug metabolism & toxicology 2007;3(6):831-45.

[33] Alfieri A, Malito E, Orru R, Fraaije MW, Mattevi A. Revealing the moonlighting role of NADP in the structure of a flavin-containing monooxygenase. Proceedings of the National Academy of Sciences of the United States of America 2008;105(18):6572-7.

[34] Shimizu M, Kobayashi Y, Hayashi S, Aoki Y, Yamazaki H. Variants in the flavin-containing monooxygenase 3 (FMO3) gene responsible for trimethylaminuria in a Japanese population. Molecular genetics and metabolism 2012;107(3):330-4.

[35] Zhang J, Tran Q, Lattard V, Cashman JR. Deleterious mutations in the flavin-containing monooxygenase 3 (FMO3) gene causing trimethylaminuria. Pharmacogenetics 2003;13(8):495-500.

[36] Basarab T, Ashton GH, Menage HP, McGrath JA. Sequence variations in the flavin-containing mono-oxygenase 3 gene (FMO3) in fish odour syndrome. The British journal of dermatology 1999;140(1):164-7.

[37] Koukouritaki SB, Simpson P, Yeung CK, Rettie AE, Hines RN. Human hepatic flavin-containing monooxygenases 1 (FMO1) and 3 (FMO3) developmental expression. PediatrRes 2002;51:236-43.

Table 1. Primer pairs employed in PCR analysis (5'→3').

Target	forward	reverse
Exon 2	GGGATTACAGGCGTGAGCTA	GCCATGGTAGCAGGTTTGGA
Exon 3	GGTAACCACGGAGGTCCTGG	GAGTTAGAGAGGCCACACTGTT
Exon 4	GCACAAGAAATCATGCAGGG	GACTTTAACAGAAGCGACCTTG
Exon 5	TGCATCTATTCACAAGGTCGCT	GATACCCTTCCCTCCTCCCC
Exon 6	AGAGTAGAAGATGTTGGGTGAG	CTCCCGGGACTAATTCCTGA
Exon 7	TCCCAATGTTGCCTCCCATC	GAGCTTTGGTGGTCTCAAG
Exon 8	CCAATTCACCTCTGTTTGGC	GAGGCATGGAGGGCTAAAACT
Exon 9	ATGTCAGGGTAGTGTGGGAA	GCTGAATAGAAAAGCAGGTGG

Figure legends

Figure 1: **Nucleotide sequences of novel *FMO3* variants in the proband**. Novel (A) and reported (B) changes in DNA sequences found in the proband. The sequences are shown only for sense strands of genomic DNA. The sequence of the complete human *FMO3* gene described in GenBank (Accession Number NG_012690.1) was used as the reference.

Figure 2. **Pedigree analysis for the presence of detected FMO3 variants in proband~~'s~~ family.** Pedigree of the child with trimethylaminuria-like phenotype and FMO3 haplotype analysis of the family. The *FMO3* gene sequence from GeneBank accession number NG_012690.1 was used as a reference sequence.

Figure 3. Trimethylamine *N*-oxygenation activities mediated by recombinant wild-type and variant FMO3 proteins. (A) Recombinant wild-type, P73L;E158K;E308G, and F140S variant FMO3 proteins expressed in bacterial membranes are shown in lanes 1–3 and 8-10 (0.25, 0.50 and 1.0 μg), 4–6 (2.5, 5.0 and 10 μg), and 11–13 (2.5, 5.0 and 10 μg), respectively. Lanes 7 and 14 show recombinant human FMO3 in insect cell microsomes commercially available (control, 0.125 pmol of FMO3). (B) Kinetic parameters for wild-type FMO3 (circles), P73L;E158K;E308G variant (triangles), and F140S variant (squares) were calculated from a fitted curve by non-linear regression (mean ± standard error, n = 8 points of substrate concentrations of 25–1000 μM) with Michaelis-Menten equations: $v = V_{max}$ [S]/(K_m + [S]).

Figure 4. Crystal structures of the AncFMO3-6 and localization of mutated residues. Panel A. Crystallographic dimer of AncFMO3-6 protein (PDB 6SE3) are shown [9]. The molecule depicting their structures is orientated as if they were sitting on the membrane (black

dashed line). Front view (left) and back view (right). In one of the monomers, ribbon representation and ball-and-stick model of FAD are visualized. E308 is shown in blue, E158 in yellow, F140 in red and P73 in green and the cofactors FAD and NAD, in cyan and orange respectively. In the other monomer, the hydrophobic shape is visualized in white. **Panel B**. P73 location and surrounding structures. *Left*. Schematic representation of the area in which P73 (CPK configuration, green) is located in the small domain of FMO3. Interactions among residues are shown as dashed lines. α-helixes are represented as red tubular structures. Residues are represented as ball-and-stick: Y469 (blue), Y74 (violet), C68 (cyan), M67 (brown), S62 (cyan) and N61 (gray). *Right*. Interactions of residues in the neighborhood of FAD in which P73 is located. Dashed lines indicate hydrophobic interactions. Residues are colored as in left. **Panel C**. Localization of F140 residue at the hydrophobic core in the big domain of FMO3. *Left*. Schematic visualization of the hydrophobic core composed by an outer wall, formed by 3 antiparallel β-sheets and an inner wall, formed by 5 parallel β-sheets. F140 (arrow) is located at the end of the outer wall projecting its R-group to the center of the core. H-bonding interactions of V110 with FAD are shown (dashed lines). *Right*. Distribution of charge around the surface of the hydrophobic core with red, white and blue representing negative, neutral and positive, respectively. F140 (arrow) is depicted as stick model (green) inside the hydrophobic core.

Fig. 1.

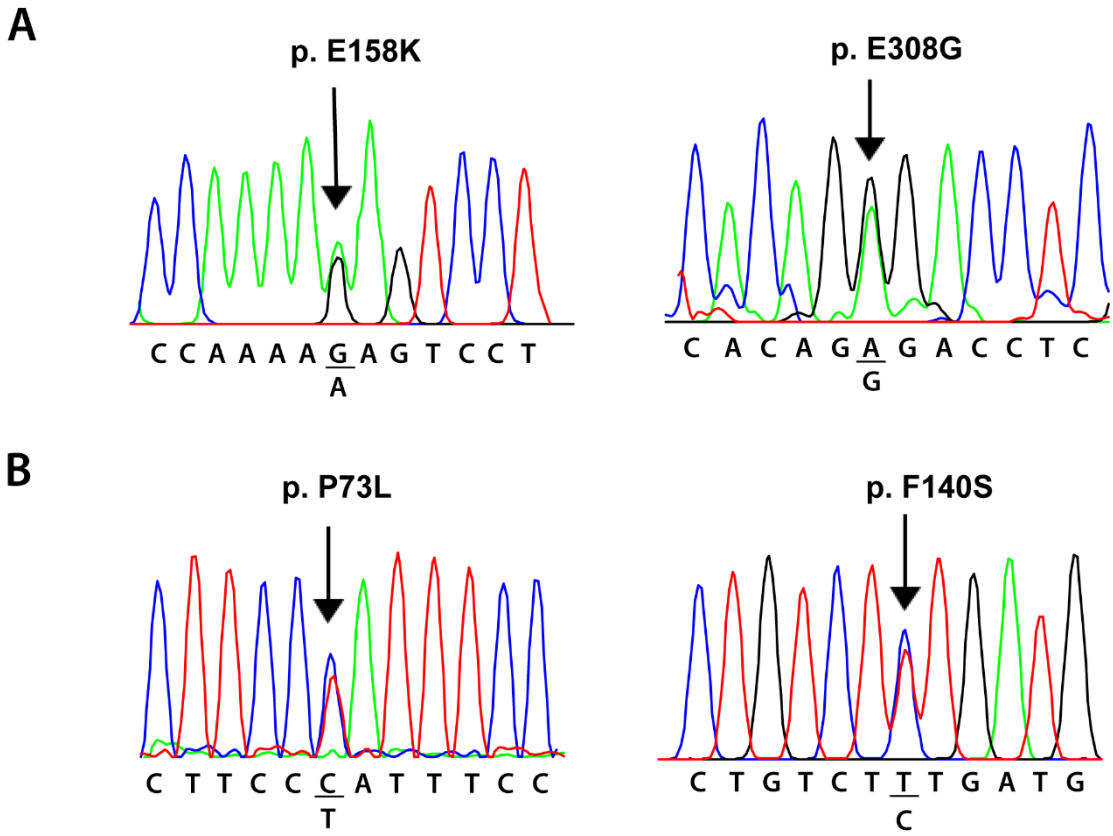
A
p. E158K
C C A A A A G A G T C C T
A
p. E308G
C A C A G A G A C C T C
G
B
p. P73L
C T T C C C A T T T C C
T
p. F140S
C T G T C T T T G A T G
C

Fig. 2

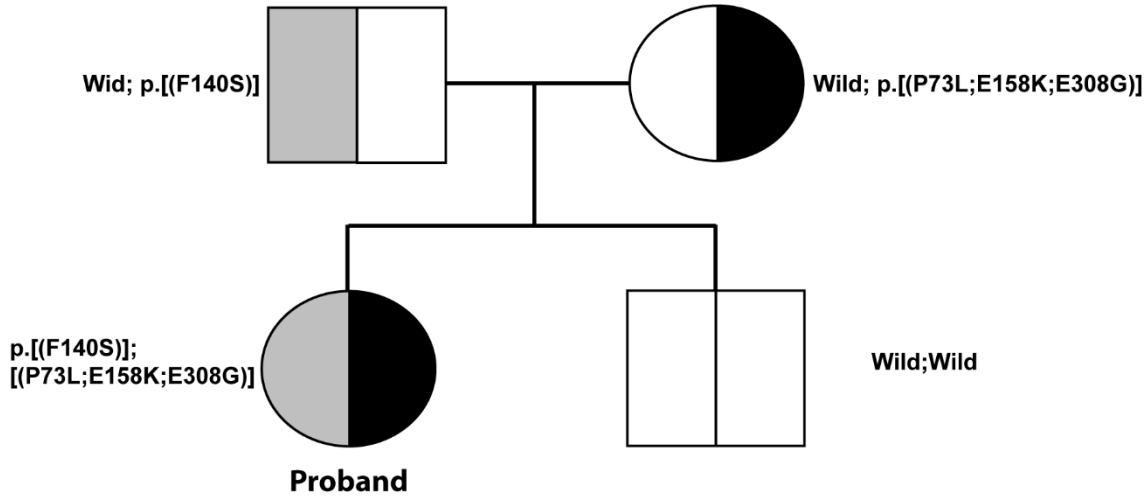

Fig. 3

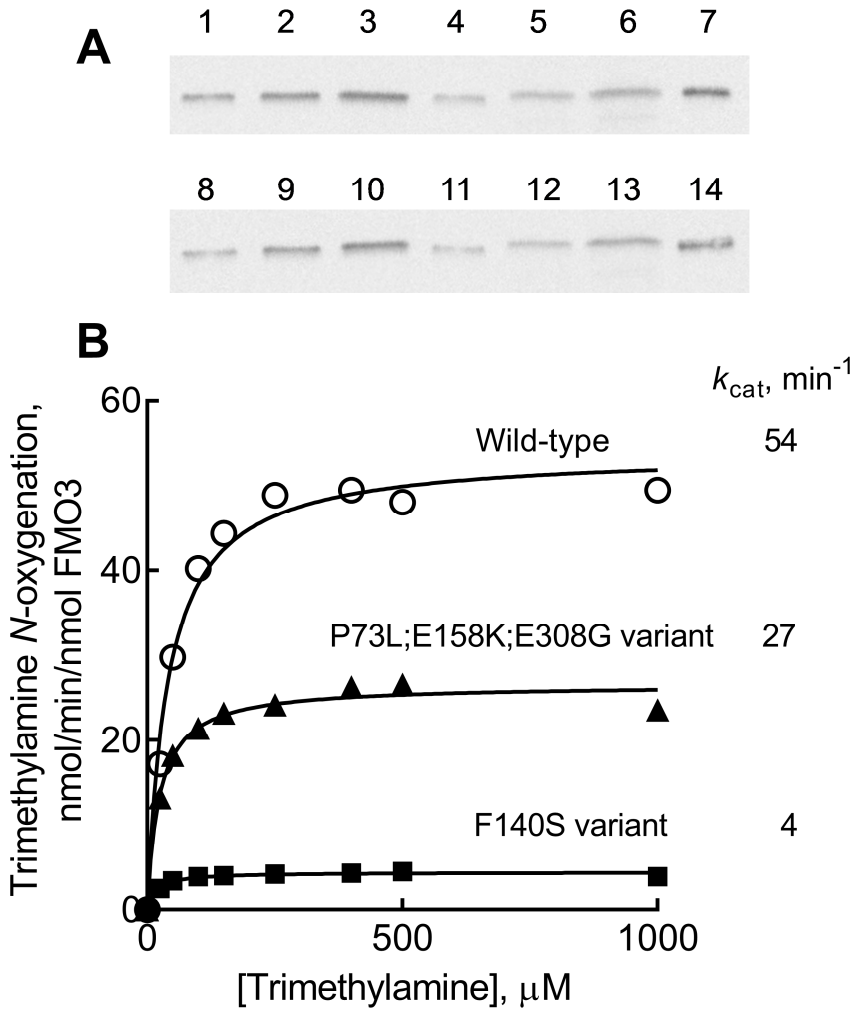
A
1 2 3 4 5 6 7
8 9 10 11 12 13 14
B
k_{cat}, min^{-1}
Wild-type 54
P73L;E158K;E308G variant 27
F140S variant 4
Trimethylamine N-oxygenation, nmol/min/nmol FMO3
60
40
20
0
0
500
1000
[Trimethylamine], μM

Fig. 4